

Blind Photographic Images Restoration with Discontinuities Preservation

Faouzi Benzarti, Hamid Amiri

National Engineering School of Tunis-Tunisia (ENIT)
Signal, Image Processing and Pattern Recognition Laboratory (TSRIF).
benzartif@yahoo.fr hamidlamiri@yahoo.com

Abstract: Image restoration is an essential pre-processing step for many image analysis and vision system applications. The task is to recover a good estimate of the original image from a blurred and noisy observation without altering and changing useful structure in the image such as discontinuities and edges. Several researches have been developed for the scalar image restoration (i.e. grayscale), but a few methods exist for the multi channel or color images. In this paper, we propose an edge-preserving regularization model that deblur and restore color images. The regularization model incorporates Partial Differential Equations (PDEs) approaches. The PDEs have remarkable advantages: they perform an anisotropic diffusion in the orthogonal direction of the gradient vector, thus preserving the natural edge of the image. To illustrate the effective performance of our edge-preserving regularization model, we present some experimental results on synthetic and photographic images.

Keywords: Photographic images, Blind deconvolution, PDE, Anisotropic diffusion, Regularization, Edge-preserving.

I. Introduction

The problem of image restoration has been extensively studied for its practical importance in image processing as well as its theoretical interest. The purpose of image restoration is to recover the original scene from the degraded observation, due to various imperfections and physical limitations in the image formation and transmission processes. This degradation often takes the form of blur and noise. The blur has many origins such as: atmospheric turbulence, camera motion, out of focus and others. In the frequency domain, the blur has a form of bandwidth filter which affects the high frequencies of the image leading to edges' image degradation. The noise may generate by: the thermal fluctuations, quantize effects and properties of communication channels. It affects the perceptual quality of the image, decreasing not only the appreciation of the image but also the performance of the task for which the image has been intended. The challenge in the image restoration is to design methods which can selectively deblur and smooth a degraded image without altering edges and losing significant features. Recently, the multichannel (e.g., color) image restoration problem has attracted much attention in the research community [15][20][21] [22]. It is well-known that

color plays a central role in digital cinematography; digital cameras; video displays; visual inspection; automatic analysis and much more. The color image processing is more complicated due to the increased dimensionality of the problem and the need to extract and exchange information from and among all bands. Mathematically, the observed degraded color channel g_i ($i=1,2,3$ for RGB color) can be modeled as a linear convolution process defined by the following equation [3]:

$$g_i = h_i * f_i + n_i \quad (1)$$

where: * denotes the convolution operator; f_i : the original color component; h_i : is the corresponding blurring kernel, known as the point spread function (PSF) in that component; n_i is the corresponding additive noise supposed to be an i.i.d Gaussian process.

Simultaneous treatment of these two types of degradation (blur and noise) by a classical linear filter is unfeasible. Indeed, since the noise resulting in high-frequency spatial fluctuations; its elimination by a low pass-filter alters the contours and produces very blurred image. In contrast, the blur is interpreted as low-frequency fluctuations; its suppression needs a high-pass filter which may amplify noise which leads to a poor quality image. Thus, the restoration is necessary to solve this kind of problem. In the standard linear image restoration, the PSF is known a priori and a long list of restoration methods had been appeared in the literature [7] [8] [13][34], such as: Inverse filtering, Wiener filtering, Least-squares filtering, Iterative image restoration and others. However, there are many situations where the PSF is not explicitly known and the true image must be identified directly from the observed image g_i by using some information about the original image and the PSF. In these cases, the blind deconvolution approach is used, which is a very important subset of image restoration [1]. Many algorithms and approaches have been proposed such as: the Iterative Blind Deconvolution algorithm (IBD) [4] [36], the Simulated Annealing algorithm (SA) [6], the NAS-RIF algorithm [2], the Anisotropic Regularization algorithm [5] and others. All these algorithms try to solve the blind deconvolution problem by minimizing an error metric which optimizes the true image and the PSF. The challenge is to find the original image from the degraded one with unknown blur

information. However, almost of these methods lead to under optimal solution and are not effective regarding to edges and discontinuities preservation. This inconvenience is primarily due to the ill-posed problem of the restoration process [10] [11] which require an adequate and robust regularization. To adopt effectively the local structures of the image and to preserve discontinuities, it should be recommended the use of a non linear regularization. Total variation (TV) regularization [18] [25] is well-known for discontinuities preservation. Recently, a new approach based on Partial Differential Equations (PDEs) [16] has emerged as a more powerful and successful approach for studying a variety of problems including image restoration, image segmentation, and image denoising. In our approach, we incorporate the PDEs as a prior model to regularize the inverse problem of restoration. The main idea is to perform an anisotropic diffusion of the color components in the orthogonal direction to the gradient of the luminance, thus preserving contours and discontinuities.

This paper is organized as follow: In section 2, we review the mathematical foundation of the PDEs regularization acting on both scalar and color images. In section 3, we present the proposed method and discuss the estimation of the model's parameters. In the last section, we exhibit the experimental results applied on both synthetic and on a real JPEG photographic images.

II. PDEs Regularization

The use of variational and PDEs methods has significantly grown and becomes an interesting research topic in the past few years. Several approaches have been proposed to tackle the problem of regularizing noisy images while preserving possible discontinuities [12][14]. These approaches have been proven to be very useful for image enhancement, restoration and segmentation. Another important advantage of the PDEs approaches is the possibility of achieving high-speed, accuracy, and stability with a great flexibility of numerical scheme resolution. In the following we will review the mathematical foundations of the PDEs regularization for the scalar images and its extension for color images.

A. Regularization in scalar images

As previously mentioned, the problem of restoration is an ill-posed inverse problem that requires a good regularization. The principle of regularization is to introduce smoothing constraints on the solution to reduce the influence of noise. Consider a spatial 2D-domain denoted by Ω with Neumann boundary conditions on $\partial\Omega$. A noisy blurred scalar image g can be regularized by minimizing the following energy functional J_λ [12] :

$$J_\lambda(f) = \int_{\Omega} (g - h * f)^2 d\Omega + \lambda \int_{\Omega} \phi(|\nabla f|) d\Omega \quad (2)$$

Where $\phi(\cdot)$ being an increasing function which controls the regularization behavior and should satisfy some conditions to ensure the edge-preserving; $|\nabla f|$ is the modulus of the image gradient; λ is a parameter that controls data smoothing. The first term in equation (2) ensures fidelity of the data; the second term imposes roughness penalty or smoothness. In the particular case of $\lambda=0$, the energy is reduced to the attached term on the data and the problem corresponds to the least-squares method which leads to an unstable solution.

Furthermore, the choice of the $\phi(\cdot)$ functions is an important point to ensure a satisfied solution. The case where $\phi(\cdot)$ has a pure quadratic form: $\phi(|\nabla f|) = |\nabla f|^2$ corresponding to a quadratic regularization or a Tikhonov regularization [10], it leads to an over-smoothed solution because high gradients at edges of the reconstructed image are penalized over-proportionally. In the remainder of this section, we will show how to choose the $\phi(\cdot)$ functions for a good compromise. Consider equation (2), any function f realizing the minima of J_λ must verify the Euler-Lagrange equations ($\nabla J_\lambda=0$), which give a necessary condition that must be verified by f to reach the minimum of J_λ , that is:

$$\frac{\partial J_\lambda}{\partial f} = \tilde{h} * (g - h * f) - \lambda \text{div} \left(\frac{\phi'(|\nabla f|)}{|\nabla f|} \nabla f \right) = 0 \quad (3)$$

Where \tilde{h} : denotes the mirror-kernel of h , $\tilde{h}(x,y)=h(-x,-y)$. We note that the divergence term in equation (3) is closely related to the anisotropic diffusion of Perona and Malik [17], with an additional term which forces the solution remaining data. By using a gradient descent algorithm with an artificial time t , equation (3) becomes:

$$\begin{aligned} \frac{\partial f}{\partial t} &= -\nabla J_\lambda = \tilde{h} * (h * f - g) + \lambda \text{div} \left(\frac{\phi'(|\nabla f|)}{|\nabla f|} \nabla f \right) \quad (4) \\ \frac{\partial f}{\partial n} &= 0 \quad \text{on } \partial\Omega \\ f(t=0) &= f_0 \end{aligned}$$

By developing the divergence term of (4), we obtain

$$\begin{aligned} \frac{\partial f}{\partial t} &= \tilde{h} * (h * f - g) + \lambda \left[\phi''(|\nabla f|) f_{\eta\eta} + \frac{\phi'(|\nabla f|)}{|\nabla f|} f_{\xi\xi} \right] \quad (5) \\ &= \tilde{h} * (h * f - g) + \lambda [c_\eta f_{\eta\eta} + c_\xi f_{\xi\xi}] \end{aligned}$$

Where: $f_{\eta\eta} = \eta^\perp H \eta$ and $f_{\xi\xi} = \xi^\perp H \xi$ are respectively the second spatial derivatives of f in the directions of the gradient $\eta = \nabla f / |\nabla f|$, and its orthogonal $\xi = \eta^\perp$; H denotes the Hessian of f . According to these definitions, on the image discontinuities, we have a diffusion along η (normal to the edge) weighted with $c_\eta = \phi''(|\nabla f|)$ and a diffusion along ξ (tangential to the edge) weighted with $c_\xi = \phi'(|\nabla f|) / |\nabla f|$. In figure1, we represent a contour C separating two homogeneous regions of the image, the isophote lines correspond to $f(x,y)=c$. In this case, the vector η is normal to the contour C , the set (ξ, η) is then a moving orthonormal basis whose configuration depends on the current coordinate point (x,y) . In the neighborhood of a contour C , the image presents a strong gradient. To better preserve these discontinuities, it is preferable to diffuse only in the direction parallel to C (i.e. in the ξ -direction). In this case, we have to annul the coefficient of $f_{\eta\eta}$ ($c_\eta=0$), and to suppose that the coefficient of $f_{\xi\xi}$ does not vanish.

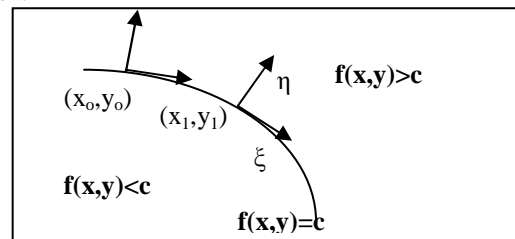


Figure 1. Image contour and its moving orthonormal basis (ξ, η)

So it appears the following conditions for the choice of the $\phi(\cdot)$ functions to be edge preserving:

$$i) \phi''(0) \geq 0 \text{ and } \phi'(0) \geq 0$$

$$ii) \lim_{|\nabla f| \rightarrow 0} c_\eta = \lim_{|\nabla f| \rightarrow 0} c_\xi = \alpha > 0$$

$$iii) \lim_{|\nabla f| \rightarrow \infty} c_\eta = \lim_{|\nabla f| \rightarrow \infty} c_\xi = 0, \text{ and } \lim_{|\nabla f| \rightarrow \infty} \frac{c_\eta}{c_\xi} = 0$$

Condition (i) avoids inverse diffusion along η and ξ . Condition (ii) allows isotropic diffusion for low gradient, with no preferred diffusion directions since η and ξ do not represent significant orientations. Condition (iii) allows anisotropic diffusion to preserve discontinuities for the high gradient. Among functions satisfies conditions -i) -ii) -iii), we choose the hyper surface function [33], while posing $u = |\nabla f|$:

$$\phi(u, k) = \sqrt{(u/k)^2 + 1} - 1 \quad (6)$$

This function introduces a parameter k or conductance parameter which acts as a gradient threshold influencing the anisotropic smoothing process. To avoid any instability in the solution, some authors suggest using a regularized (or smoothed) version of the image gradient, in which the gradient of f is replaced by [14]:

$$\nabla f_\delta = \nabla(G_\delta * f) \quad (7)$$

where G_δ is a Gaussian with standard deviation δ .

Moreover, the hyper surface function (6) presents the particularity to be convex which simplifies the optimization procedure. Equation (4) can be solved numerically by using a gradient descent method, in which we substitute $\partial f / \partial t$ with the discrete difference $(f^{n+1} - f^n) / \Delta t$ [29], the step time Δt must be chosen less than 0.25 to ensure the stability of the PDE. This leads to the following iterative equation:

$$f^{n+1} = f^n + \Delta t [\tilde{h} * (h * f - g) + \lambda \operatorname{div}(\frac{\phi'(|\nabla f_\delta^n|, k)}{|\nabla f_\delta^n|} \nabla f_\delta^n)] \quad (8)$$

Basically such PDEs regularization should adapt its diffusion behaviour to the local geometry of the image defined by the edge indicators and edge orientations.

B. Regularization in color images

In this subsection, we will extend the PDEs regularization seen previously to the color images. In general, the color image can be expressed by the RGB color system, in which we define a vectorial application $I(x, y) : \Omega \subset \mathbb{R}^2 \rightarrow \mathbb{R}^3$ which associates to pixel $(x, y) \in \Omega$, its three component values in the RGB color space:

$$\vec{I}(x, y) = \begin{bmatrix} I_1(x, y) \\ I_2(x, y) \\ I_3(x, y) \end{bmatrix} = \begin{bmatrix} I_R(x, y) \\ I_G(x, y) \\ I_B(x, y) \end{bmatrix} \quad (9)$$

The simplest way to process color images is to consider each color components independently of the others. Unfortunately, this solution is not optimal because the strong correlation among channels. Another approach is to reduce the dimensionality of the vector image to a scalar one by evaluating the luminance function given by: $f(I) = \sum_{i=1}^M I_i^2$, with the corresponding gradient norm $N = \|\nabla f(I)\|$ and the

direction $\theta_+ = \nabla f(I) / \|\nabla f(I)\|$. However, this luminance function is not being able to detect iso-luminance contours. To overcome these problems, we propose using Di Zenzo's gradient norm [20][14] which is based on the surfaces differential geometry. It consists on defining a multispectral tensor associated to a vector field [35]. This allows looking for the local variations in the image. Considering the differential vector dI [23]:

$$dI = \frac{\partial I}{\partial x} dx + \frac{\partial I}{\partial y} dy \quad (10)$$

The vector norm corresponds to:

$$\|dI\|^2 = dI^T dI = \begin{bmatrix} dx \\ dy \end{bmatrix}^T \begin{bmatrix} s_{11} & s_{12} \\ s_{21} & s_{22} \end{bmatrix} \begin{bmatrix} dx \\ dy \end{bmatrix} \quad (11)$$

$$s_{i,j} = \sum_{k=1}^3 \frac{\partial f_k}{\partial x_i} \frac{\partial f_k}{\partial x_j} \quad 1 \leq i, j \leq 2,$$

With f_k : k^{th} component channel.

The structure tensor $[s_{ij}]$ defines the local variations of the color image I and has the corresponding eigenvalues [29]:

$$\alpha_+ = \frac{s_{11} + s_{22} + \sqrt{(s_{11} - s_{22})^2 + 4s_{12}^2}}{2} \quad (12)$$

$$\alpha_- = \frac{s_{11} + s_{22} - \sqrt{(s_{11} - s_{22})^2 + 4s_{12}^2}}{2}$$

The orthogonal eigenvectors (in the algebraic sense) θ_+ and θ_- are the corresponding variation orientations:

$$\theta_+ = \frac{1}{2} \arctan\left(\frac{2s_{12}}{s_{11} - s_{22}}\right) \quad (13)$$

$$\theta_- = \theta_+ + \frac{\pi}{2}$$

The highest eigenvalue of the multispectral tensor then corresponds to the square norm of the gradient.

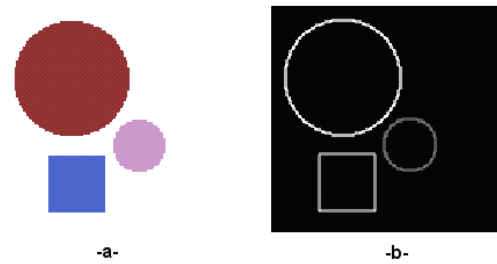


Figure 2. Illustration of the color gradient; -a- original color image; -b- Norm color gradient ($|\nabla I| = \sqrt{\alpha_+ - \alpha_-}$).

An appropriate choice for the norm of the gradient will:

$$|\nabla I| = \sqrt{\alpha_+ - \alpha_-} \quad (14)$$

These indicators of discontinuities as illustrated in figure 2 contribute to the anisotropic diffusion process; that is isotropic smoothing is allowed when $\alpha_+ \sim \alpha_-$, and to carry out a directional diffusion (in the θ_- direction) when $\alpha_+ \gg \alpha_-$ (i.e. discontinuities).

The iterative deconvolution process is derived from the Perona-Malik PDEs [17] which is extended to the three component color image f_i , that is:

$$f_i^{n+1} = f_i^n + \Delta t [\tilde{h}_i * (g_i - f_i^n * h_i) + \lambda \operatorname{div} \left(\frac{\phi'(|\nabla f_i^n|, k) \nabla f_i^n}{|\nabla f_i^n|} \right)] \quad (15)$$

Where \tilde{h} : denotes the mirror-kernel of h , $\tilde{h}(x,y)=h(-x,-y)$. $\phi(\cdot)$ being an increasing function which controls the regularization behavior and should satisfy some conditions to ensure the edge-preserving [14][19]; $|\nabla f|$: denotes the norm of the color gradient which derived from (14). However, the unknown blur h_i makes the equation more complicate. Indeed the blur is closely related to color bands. To reduce this complexity, we assume a spatio-spectral invariance of the blur that is $h_i = h$ for all bands. We have to note that this approximation is valid in the case of relatively small blur.

III. Proposed method

The proposed method is based on three main steps, as summarized in figure 4: First, the blur is estimated from the grayscale version of the degraded color image. Second, the norm of the color gradient is estimated and updated from the feedback of the three estimated color bands. Third, the iterative procedure of equation (15) is used, in order to restore the three spectral bands (f_R, f_G, f_B) of the original color image. In the following, we will give more details description of estimating the blur and the model's parameters.

A. Blur estimation

We propose applying an iterative blind deconvolution based on the Richardson algorithm [26] which is widely used for restoring astronomical images [27]. The algorithm follows an iterative procedure, alternating between the estimate of the image f and the estimate of the blur h . After initialization of the variables f and h , where $f = g$ and $h = \delta$ (unity impulse), we have [9]:

$$\hat{h}^{n+1} = \frac{\hat{h}^n}{\sum \hat{f}^n} \left[\hat{f}^n \frac{g}{\hat{h}^n * \hat{f}^n} \right] \quad (16)$$

$$\hat{f}^{n+1} = \frac{\hat{f}^n}{\sum \hat{f}^n} \left[\hat{h}^n * \frac{g}{\hat{h}^n * \hat{f}^n} \right]$$

The stopping criterion is given by the relative norm error (RNE) :

$$\frac{\|\hat{h}^{n+1} - \hat{h}^n\|^2}{\|\hat{h}^n\|^2} \leq 10^{-4} \quad (17)$$

where \hat{h} : denotes the estimated blur which is related to the original blur by $\hat{h} = h + \Delta h$, with Δh the error of estimation. Obviously, this method can also estimate the original image, but the problem lays in the Gibbs oscillations nearly discontinuities in the restored image.

B. Parameters estimation

The image quality is widely depending on the parameters (λ, k), known as hyperparameters. These parameters are dependent on each other and may lead to different results if chosen inappropriately. The conductance parameter k in the $\phi(\cdot)$ function must be chosen carefully. If its value is too large, the diffusion process will over-smooth and leads to a

blurred image. In contrast, if its value is too small, the diffusion process will stop the smoothing. To avoid this difficulty and obtaining an optimal value of k , we propose using a robust statistical measure 'the Median Absolute Deviation' (MAD) [28] [30]:

$$k = 1.482 \operatorname{MAD}(|\nabla f|) \quad (18)$$

$$\operatorname{MAD}(|\nabla f|) = \operatorname{median}(\operatorname{norm}(|\nabla f|) - \operatorname{median}(|\nabla f|))$$

Where f : is the grayscale version of the image. Areas in which the gradient magnitude is lower than k will be blurred more strongly than areas with a higher gradient magnitude. This tends to smooth uniform regions, while preserving the edges. The choice of the regularization parameter λ is a crucial and a difficult problem in the theory of regularization. This parameter controls the closeness to the data versus the prior knowledge of the solution. Too small values of λ yield overly oscillatory estimates owing to either noise or discontinuities; too large values of λ yields over smoothed estimates. The optimal choice of λ can be obtained by considering the blur signal to noise ratio (BSNR) [13]:

$$\lambda = \frac{1}{\operatorname{BSNR}} \quad (19)$$

$$\operatorname{BSNR} = 10 \log_{10} \left(\frac{\operatorname{Var}(y)}{\sigma^2} \right)$$

where $\operatorname{Var}(y)$ and σ^2 : denote respectively the variance of the blurred image and the variance of the additive white Gaussian noise (with standard deviation σ). To estimate the noise's variance, we propose using the Discrete Wavelet Decomposition (DWT) [31] which provides an appropriate basis for separating noisy signal from the image signal. By applying DWT, the image is divided into four sub-bands as illustrated in figure 3 (LL1, LH1, HL1, and HH1), arise from separable applications of vertical and horizontal filters.

LL2	HL2	HL1
LH2	HH2	
LH1		HH1

Figure 3. Illustration of two levels DWT decomposition

The sub-bands labeled LH1, HL1 and HH1 represent the finest scale wavelet coefficients (i.e. detail) while the subband LL1 corresponds to coarse level coefficients (i.e. approximation). The variance σ^2 is then estimated from the subband HH1 in the first scale [32]:

$$\sigma^2 = \frac{\operatorname{median}(|Y_{ij}|)}{0.6745} \quad (20)$$

Where Y_{ij} : wavelet coefficients in the sub-band HH1.

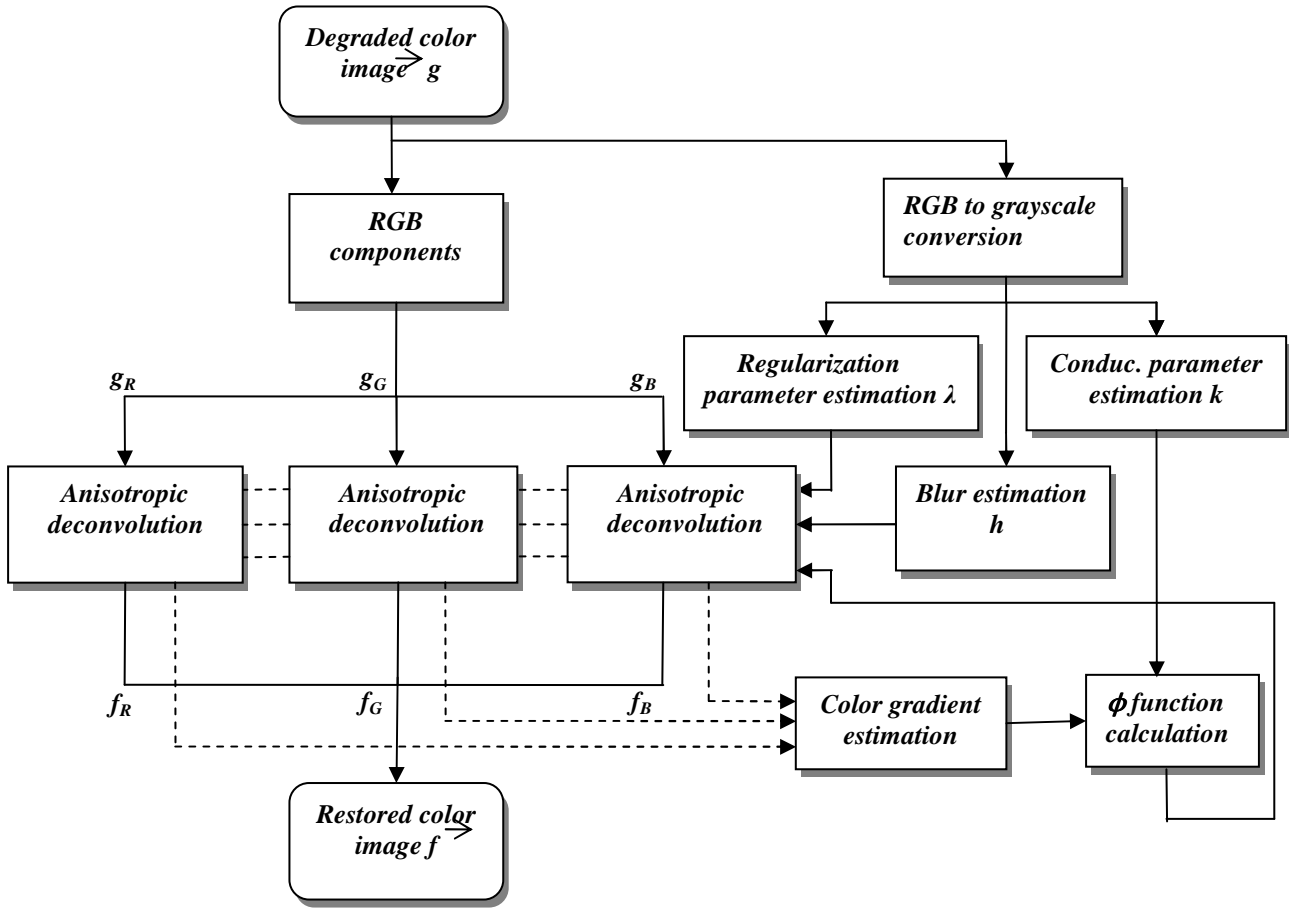


Figure 4. Block diagram of the proposed method

IV. Experimental results

In this section, we present the numerical results illustrating the efficiency and the effectiveness of the proposed algorithm. To evaluate the color image quality in the simulation tests, we use an objective measure PSNR defined by:

$$PSNR = 10 \log_{10} \frac{(N_{\max})^2}{MSE} \quad (21)$$

where N_{\max} : the maximum fluctuation in the input image, $N_{\max} = 255$ when the components of a pixel are encoded on 8 bits; MSE: denotes the Mean Square Error, given by:

$$MSE = \frac{1}{3MN} \sum_{i=1}^M \sum_{j=1}^N \sum_{m=1}^3 |f_m(i, j) - \hat{f}_m(i, j)|^2 \quad (22)$$

where f_m : the original color image components indexed by m ($m = 1, 2, 3$), \hat{f}_m : the restored image components. Clearly this objective measure can be used only in simulation, since it uses the original image in its computation.

In the first experimental, we test the performance of the algorithm with an artificially generated blurred image sized 128x128 pixels, figure 5.b, obtained by convolving a Gaussian blur sized 5x5 and added with a zero-mean Gaussian noise, having SNR=14.58 dB. The initialized parameters are fixed to: $N=450$ (the number of iterations) and $\Delta t=0.24$. The model's parameters are estimated to: $k=0.31$, $\lambda=0.63$. The restored image figure 5.c, shows a significantly improvement. The edges and discontinuities have been recovered and preserved with a good suppression of noise. In figures 5.d, 5.e, 5.f, 5.g, we present the original and the estimated blur by using the iterative alternating procedure in equation (16). The result is satisfactory; the original blur is well estimated. The second test was performed with the same image by using a mean filter which simulates an out of focus blur h sized 3x3:

$$h = \frac{1}{9} \begin{bmatrix} 1 & 1 & 1 \\ 1 & 1 & 1 \\ 1 & 1 & 1 \end{bmatrix} \quad (22)$$

And added with a Gaussian noise having SNR=10.68 dB. The model's parameters are estimated to: $k=0.56$, $\lambda=0.81$. As shown in figure 6, the proposed approach shows that the image and the PSF can be recovered even under the presence of high noise level and blur.

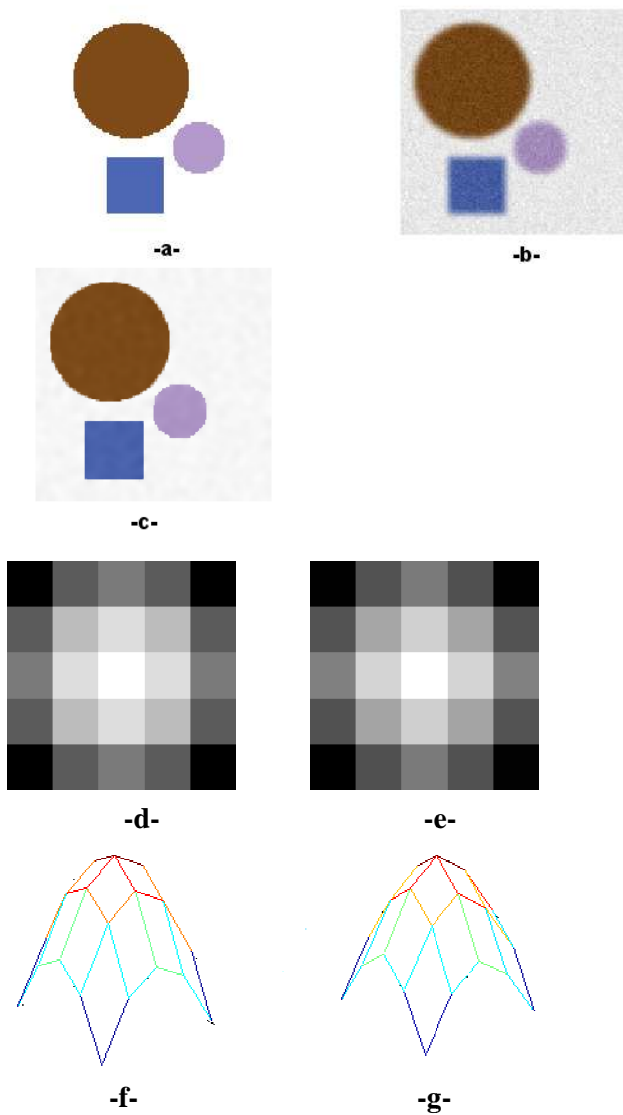


Figure 5. Gaussian blur simulation; -a- Synthetically image;-b- Blurred and noisy image; -c- Restored image with PSNR=26.57 dB; -d- Original PSF;-e- Estimated PSF with RNE=0.85 10^{-4} ;-f- Mesh plot of the original PSF;-g- Mesh plot of the estimated PSF

In the following, we will compare our proposed model to some existing methods such as: the Fast Total Variation algorithm (FTV) [24]; the Wiener approach [13], the Lucy-Richardson algorithm [27], the Constrained Least Square (i.e. regularized filter) [8], the iterative blind deconvolution (IBD) [4]. In this test, we simulate an out-of-focus blur (i.e. mean filter sized 3x3) in a photographic image added with a Gaussian noise (SNR=27.12dB). Recall that the results are compared in terms of noise reduction and discontinuities preservation. The model's parameters are estimated to: $k = 0.11$, $\lambda = 0.57$. The results in figure 7 show that our method and the TV one have similar performance. They can successfully remove noise and blur and produce good quality image. Nevertheless, our method seems to better preserve and enhance discontinuities as shown (especially on the leaves hues). The other methods lead to under optimal solution and are not effective regarding to edges and

discontinuities preservation. They remove the blur but introduce Gibbs oscillations with a heavily amplified noise. It should be noted that the image quality is very sensitive to the PSF's support initialization and especially to the parameter of regularization.

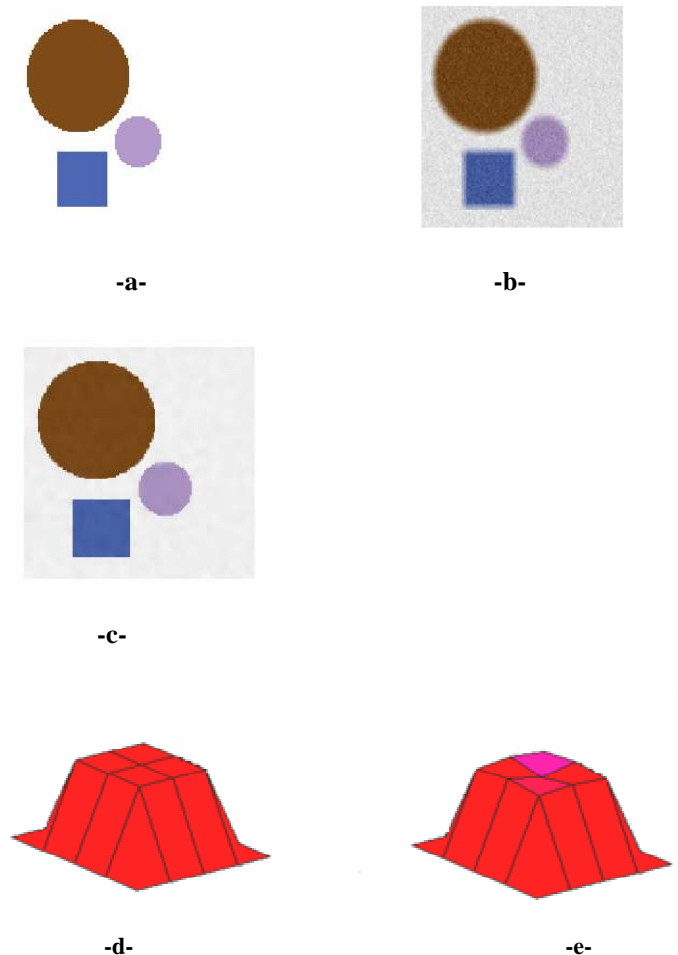


Figure 6. Out of focus blur simulation; -a- Synthetically image; -b- Degraded image;-c- Restored image with PSNR=27.61 dB; -d- Mesh plot of the original PSF;-e- Mesh plot of the estimated PSF with RNE=0.32 10^{-4} .

The assumption of a Gaussian noise to estimate the latter is not always true in a real case; it is sometimes useful to make a manual refinement of this parameter to avoid sub-optimal solution. Obviously the visual quality image decision is always subjective.

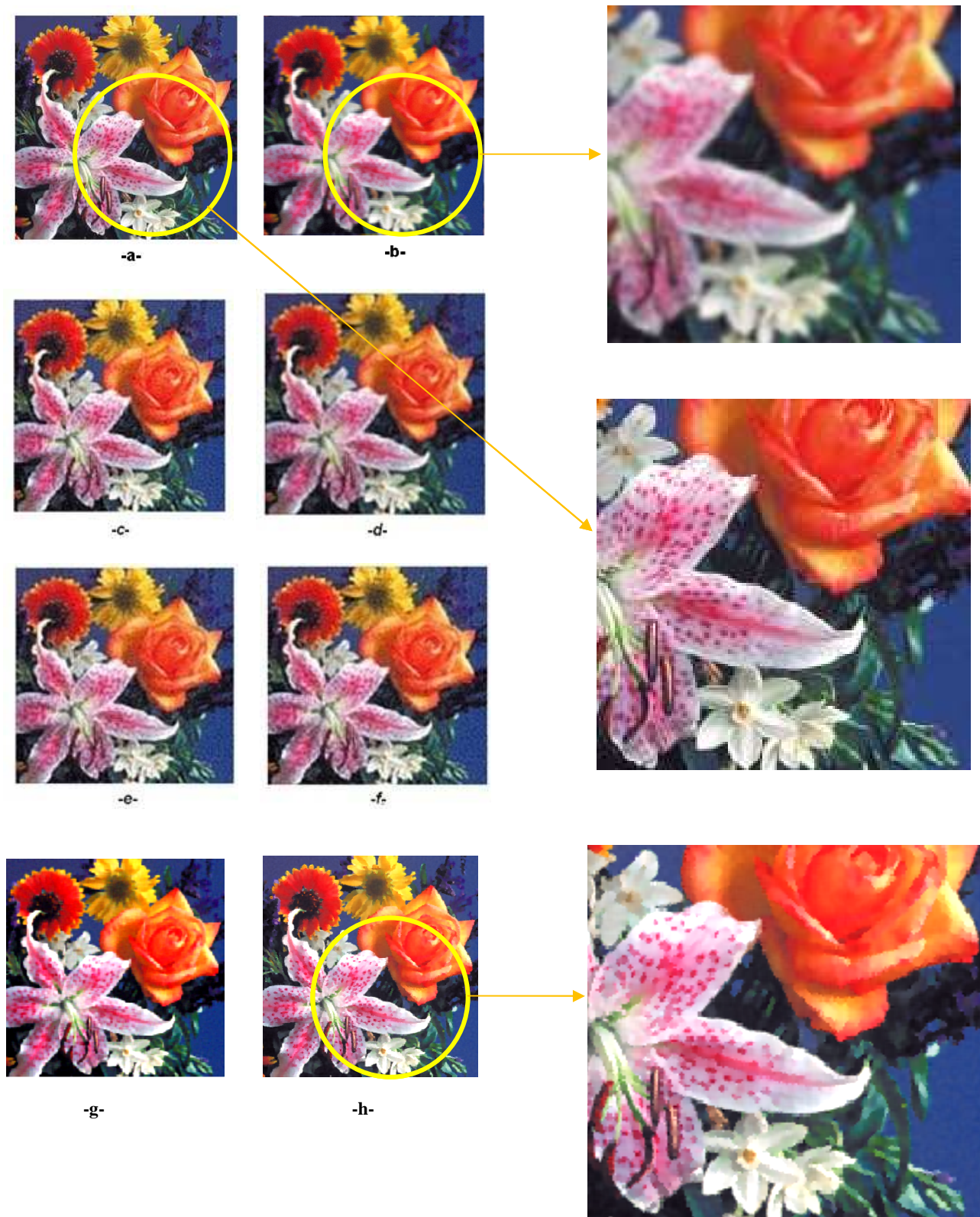


Figure 7. Out of focus blur simulation; -a- Original image with details zoom; -b- Degraded image with details zoom; -c- Wiener Deconvolution, PSNR=21.86dB; -d- Richardson deconvolution, PSNR=18.64dB; -e- The Constrained Least Square, PSNR=21.08 -f- The iterative blind deconvolution (IBD) PSNR=19.24 dB; -g- Fast TV deconvolution ,PSNR=23.05dB; -h- Proposed method with details zoom, PSNR=23.74dB.

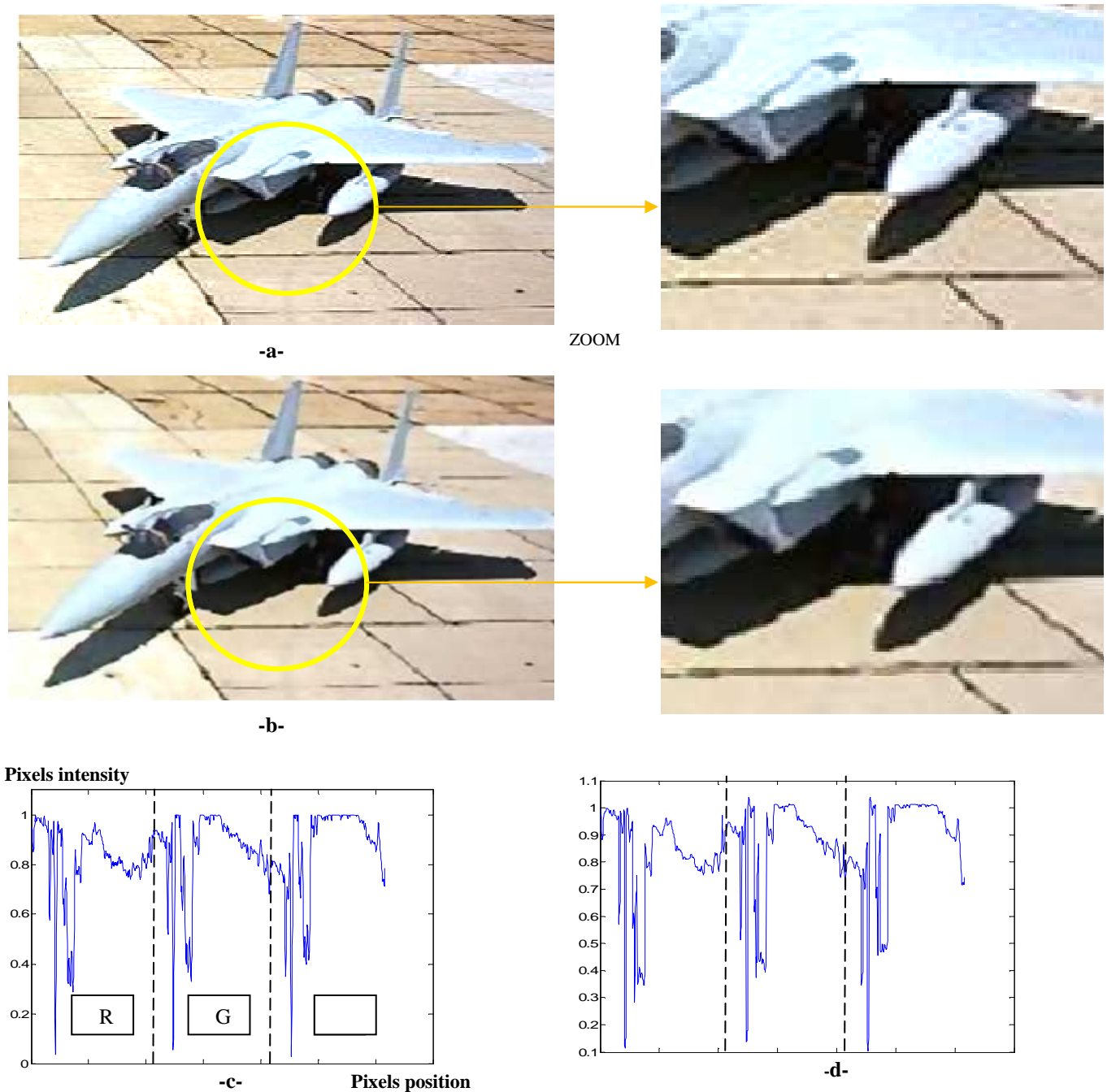


Figure 8. JPEG image test; -a- Original image with its details zoom; -b- Restored image with its details zoom; -c - Original image cross-section through the RGB components (Row=100 pixels) ; -d- Cross-section for restored image

We also test the performance of the algorithm on a JPEG real photographic image figure 8 (from the Web site) sized 238x411. This image seems to be noisy and poor quality. For the algorithm we initialized the PSF's support to 3x3 size and the number of iterations $N=850$; the PSF's support initialization and especially to the parameter of regularization. The assumption of a Gaussian noise to estimate the latter is not always true in a real case; it is sometimes useful to make a manual the model's parameters are estimated to: $k = 0.23$, $\lambda = 0.56$. As shown in figures 8.b, the restored image has a good quality with significantly enhanced edges. A cross-sectional analysis of the image in figure 8.d, shows that the noise and

the artefacts have been reduced. It should be noted that the image quality is very sensitive to refinement of this parameter to avoid sub-optimal solution. Obviously the visual quality image decision is always subjective.

V. Conclusion

In this paper, we have proposed an edge-preserving regularization model that deblurs and restores color image. This approach has the particularity to associate deconvolution and anisotropic diffusion. This allows a great flexibility of processing and contributes to: eliminate the blur, reducing noise and preserving natural edges of the image. Color images processing is not a trivial task because the strong inter-band

correlation. The anisotropic diffusion is well suited for scalar images; its extension to color images, needs the use of the differential geometry of surfaces formalism. This formalism allows defining a common tensor gradient to represent the image's discontinuities on each spectral band. Experimental results on synthetic and digital picture are very promising and provide very good quality images in terms of noise reduction and discontinuities preservation. This approach has been tested with a particular case of a Gaussian and an out of focus blur, but can be generalized for any kind of blur and other applications. Future works will include multispectral images other than RGB space and an adaptive locally parameters estimation.

References

- [1] D. Kundur, and D. Hatzinakos, "Blind image deconvolution", *IEEE Signal Processing Magazine*, vol. 13(3), pp. 43-64, 1996.
- [2] D. Kundur, and D. Hatzinakos, "A Novel blind deconvolution scheme for image restoration Using Recursive Filtering", *IEEE Trans. Signal Processing*, vol. 46, pp. 375-390, 1998.
- [3] R.C. Gonzalez, *Digital Image Processing*, Second Edition, Prentice Hall, 2002.
- [4] G.R. Ayers and J.C. Dainty, "Iterative blind deconvolution Method and Its Applications", *Optics Letters*, vol. 13(7), pp. 547-549, 1988.
- [5] Y.-L. You and M. Kaveh, "Anisotropic blind image restoration", *IEEE International Conference on Image Processing*, Lausanne, Switzerland, vol. 2, pp. 461-464, 1996.
- [6] M.C. McCallum, "Blind deconvolution by simulated annealing", *Optics Communications*, vol. 75(2), pp. 101-105, 1990.
- [7] Michael K. Ng, Andy C. Yau, "Super-resolution image restoration from blurred low-resolution images", *Journal of Mathematical Imaging and Vision*, vol. 23(3), pp. 367-378, 2005
- [8] A.K Katsaggelos, "Iterative image restoration algorithm", *Optical Engineering*, vol 28(7), pp. 735-748, 1989,.
- [9] D.S.C. Biggs, M. Andrews, "Acceleration of iterative image restoration algorithms", *Applied Optics*, vol. 36(8), 1997.
- [10] A. Tikhonov, V. Arsenin, *Solution of Ill-Posed Problems*, John Wiley and Sons, 1977.
- [11] J. Hadamard, *Lectures on the Cauchy Problem in Linear Partial Differential Equations*, Yule University Press, 1923.
- [12] S. Teboul, L. Blanc-Féraud, G. Aubert, M. Barlaud, "Variational approach for edge-Preserving regularization using coupled PDE's", *IEEE Trans. Image Processing*. Vol 7(3), 1998.
- [13] M.R. Banham, A.K Katsaggelos, "Digital image restoration", *IEEE Signal Processing Magazine*, vol. 14(2), pp. 24-41, 1997.
- [14] D. Tschumperlé, R. Deriche, "Vector-valued image regularization with PDEs: a common framework for different applications", *IEEE Trans. On Pattern Analysis and Machine Intelligence*, vol. 27(4), 2005.
- [15] P. Blomgren, T. Chan, "Color TV total variation methods for restoration of vector valued images," *IEEE Trans. Image Processing*, vol 7:, pp. 304-309, 1998.
- [16] T.F. Chan, J.J. Shen, "Image Processing and Analysis-Variational, PDE, Wavelet, and Stochastic Methods", *SIAM*, Philadelphia, 2005.
- [17] P. Perona and J. Malik, "Scale-space and edge detection using anisotropic diffusion," *IEEE Trans. Pattern. Anal. Machine Intell.*, vol. 12, pp. 629-639, 1990.
- [18] L. I. Rudin, S. Osher, and E. Fatemi, "Nonlinear total variation based noise removal algorithms", *Phys. D*, vol. 60: 259-268, 1992.
- [19] G. Sapiro and D. Ringach, "Anisotropic diffusion of multivalued images with applications to colorfiltering", *IEEE Trans. Image Processing*, vol. 5, pp. 1582-1586, 1996.
- [20] S. Di Zenzo, "A note on the gradient of the multi-image", *Computer Vision, Graphics, and Image Processing*, vol 33(1), pp. 116-125, 1986.
- [21] T. F. Chan, S. H. Kang, and J. Shen, "Total variation denoising and enhancement of color images based on the CB and HSV color models", *Journal of Visual Communication and Image Representation*, vol. 12, pp. 422-435, 2001.
- [22] H. J. Trussell, E. Saber, and M. Vrhel, "Color image processing," *IEEE Signal Processing Magazine*, vol. 22(1), pp. 14-22, 2005.
- [23] G. Aubert, P. Kornprobst, *Mathematical Problems in Image Processing*, Applied Mathematics Sciences, Springer-Verlag, New York, 2002.
- [24] J. Yang, W. Yin, Y. Zhang and Y. Wang, *A Fast Algorithm for Edge-Preserving Variational Multichannel Image Restoration*, Tech. Report, TR08-09, 2008, CAAM, Rice University, 2008.
- [25] D. Strong, T. Chan, "Edge-preserving and scale-dependent properties of total variation regularization, *Inverse Problems*", *Inverse problems*, vol. 19, pp. 165-187, 2003.
- [26] W.H. Richardson, "Bayesian Based Iterative Method of Image Restoration", *JOSA*, vol. 62(1), pp. 55-59, 1972.
- [27] L.B. Lucy, "An iterative technique for the rectification of observed distribution", *Astronomical Journal*, vol. 76(6), pp. 745-754, 1974.
- [28] P.J. Rousseau, A.M. Lerroy, *Robust Regression and Outlier Detection*, Newyork, Wiley 1987.
- [29] J. Weickert, *Anisotropic diffusion in Image Processing*, B.G. Teubner, 1998.
- [30] M. J. Black, G. Sapiro, *Edges as Outliers: Anisotropic Smoothing Using Local Image Statistics*, Lecture Notes in Computer Science, Springer, Berlin, Germany, 1999.
- [31] S.G. Mallat, "A theory for multiresolution signal decomposition: the wavelet representation", *IEEE PAMI*, vol 11(7):674-693, 1989.
- [32] D.L. Donoho, I.M. Jonsthone, "Ideal Spatial adaption via wavelet shrinkage", *Biometrika*, Vol 81(3), pp 425-445, 1994.
- [33] P. Charbonnier, G. Aubert, M. Blanc-Féraud, and M. Barlaud, "Two deterministic half-quadratic regularization algorithms for computed imaging". *Proceedings of the International Conference on Image Processing*, Vol.2, 168-172, 1994.
- [34] R.C. Gonzalez, R.E. Woods, S.L. Eddins, *Digital Image Processing Using MATLAB*, Prentice Hall; edition 2003.
- [35] H. Yoo; B. Kim; K. Sohn; "Coherence enhancing diffusion filtering based on connected component analysis structure tensor"; 6th *IEEE Conference on Industrial Electronics and Applications (ICIEA)*; pp. 271- 274 ; 2011.
- [36] Fahmy, M.F.; Abdel Raheem, G.M.; Mohammed, U.S.; Fahmy, O.F.; "A Fast Iterative Blind image restoration algorithm" 28th *IEEE Conference on National Radio Science Conference (NRSC)*; pp1-8, 2011.

Authors Biographies



Mr Faouzi Benzarti received his Engineer's degree in Electrical Engineering from the National Engineering School of Monastir (TUNISIA) in 1987, and his master's degree in Biomedical Engineering from the Polytechnic School of Montreal CANADA in 1991. He obtained his Ph.D degree from the National Engineering School of Tunis (ENIT) in 2006. He is presently an assistant professor in the High School of Technology and Science of Tunis (ESSTT) and a member of research group in the Image Processing, Signal and Pattern Recognition TSRIF Laboratory. His current researches include: Image Deconvolution, Image Inpainting, Anisotropic diffusion, Image retrieval, 3D Biometry.



Mr Hamid Amiri received the Diploma of Electro-technics, Information Technique in 1978 and the PHD degree in 1983 at the TU Braunschweig, Germany. He obtained the Doctorates Sciences in 1993. He is presently a Professor at the National Engineering School of Tunis (ENIT) Tunisia. From 2001 to 2009 he was at the Riyadh College of Telecom and Information. Currently, He is now the head member of research group in the Image, Signal and Pattern Recognition Laboratory. His research is focused on Image Processing, Speech Processing, Document Processing and Natural language processing.